Analysis of Aircraft Attitude Control Systems Prone to Pilot-Induced Oscillations

Ronald A. Hess*
University of California, Davis, California

An optimal control model of the human pilot is applied to the study of aircraft attitude control systems. Attention is focused upon documented examples where an aircraft's linear pitch attitude dynamics have led to the incidence of pilot-induced oscillations. In particular, the effects of control system time delays, or higher-order vehicle dynamics that can be represented by time delays, are examined. A simple criterion for determining an aircraft's susceptibility to pilot-induced oscillations is offered. The criterion is based upon the open-loop pilot/vehicle crossover frequency as predicted by the optimal control model. The modeling procedure offers insight into the manner in which higher-order vehicle dynamics effect pilot equalization requirements and closed-loop pilot/vehicle performance.

Introduction

THE advent of modern, digital stability and control augmentation systems has created a renewed interest in the study of the handling qualities associated with aircraft attitude control. This renewed interest is attributable to two factors. First, the higher-order nature of the dynamics typically associated with digital control systems make analytical prediction of handling qualities difficult. Past handling qualities specifications[1] were written assuming "classical" aircraft characteristics, e.g., in the longitudinal mode, the existence of distinct and dominant short-period dynamics was assumed. With modern systems, the short-period characteristics may be dramatically altered by feedback and the higher-order control system dynamics themselves may dominate the vehicle handling qualities. Second, shortcomings in predictive techniques are made even more critical by the fact that severe handling qualities deficiencies often arise in practice that are directly attributable to the higher-order nature of the control law being digitally implemented. An example of this is the ability of high-frequency phase lags or time delays in the control system to sharply degrade aircraft handling qualities and to be a contributing factor to pilot-induced oscillations (PIO).[2]

In the research to be described, a pilot modeling technique for handling qualities research, introduced in Ref. 3, is utilized and extended to cover flight control systems with time delays. The delays can be either real or a realistic representation of the low-frequency phase effects of high-frequency control system dynamics. Particular emphasis is placed upon analyzing flight test results where control system dynamics and time delays have been recognized as contributing to PIO. A model-based criterion for predicting an aircraft's susceptibility to PIO is offered and applied to a test case involving the Shuttle Orbiter vehicle in a landing approach configuration.

Background

The optimal control model (OCM) of the human pilot, introduced in Ref. 4, had its genesis in the hypothesis that, with limitations and in specific well-defined control tasks, the human pilot can be described in terms of the operation of a linear optimal estimator and regulator. This hypothesis led quite naturally to the application of linear-quadratic-Gaussian (LQG) estimation and control techniques to the description of human control behavior and to the OCM validation reported in Ref. 4. Since the appearance of Ref. 4, the OCM has been used to study a variety of manual control problems pertinent to aircraft, e.g., see Ref. 5.

For the single-axis tasks to be discussed here, the dynamics of the regulator part of the OCM formulation are dominant. This is fortunate, for it allows a brief tutorial review of optimal regulator design to summarize the technique for selecting the all-important OCM index-of-performance weighting coefficients for single-axis attitude regulation tasks. This technique relies only upon the transfer function of the vehicle's attitude dynamics, including the control system.

Consider the longitudinal tracking of Fig. 1, in which the pilot is attempting to minimize pitch attitude deviations $\theta(t)$ in the presence of atmospheric disturbances. Ignore the dashed line for the present. We will eventually model the pilot in this task with the complete OCM, i.e., a combined regulator and estimator. The separation principle associated with the LQG formulation allows us to attack these problems separately. Since we have indicated that the equalization characteristics of the regulator are quite similar to those of the complete OCM (and hence, the pilot) in single-axis tasks, we will initially concentrate upon the characteristics of a deterministic regulator designed to maximize the transient performance of the single-axis system shown in Fig. 1. A reasonable index of performance for this task is

$$J=\frac{1}{T_0}\int_0^{T_0}[\theta^2(t)/\theta_M^2+\dot{\delta}^2(t)/\dot{\delta}_M^2]\,dt \tag{1}$$

The pilot is assumed to generate a control input $\delta(t)$, defined as the product of a feedback gain matrix and the state vector, which minimizes a weighted sum of mean square tracking error and control rate. The weighting coefficients in Eq. (1) have been expressed as the inverse of the square of "maximum allowable" deviations of the error and control rate.[6]

One can determine the feedback gains that minimize the index of performance of Eq. (1) for a specific set of vehicle/control system dynamics. Let us consider three simple stereotypes for these dynamics,

$$Y_{c_1}=K, \qquad Y_{c_2}=K/s, \qquad Y_{c_3}=K/s^2 \tag{2}$$

These dynamics are pertinent to this discussion since they have shown to induce three fundamental types of equalization

Presented as Paper 81-1771 at the AIAA Guidance and Control Conference, Albuquerque, N. Mex., Aug. 19-21, 1981; submitted Oct. 6, 1981; revision received March 8, 1983.

*Associate Professor, Department of Mechanical Engineering. Member AIAA.

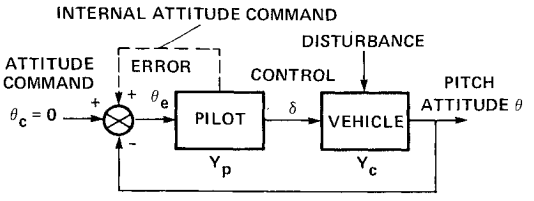

Fig. 1 Pitch attitude regulation task.

in the human (integral, proportional, and derivative in the region of open-loop crossover for Y_{c_1}, Y_{c_2}, and Y_{c_3}, respectively).[7] They also coincide with the dynamics used in developing both modern and classical representations of the human pilot, e.g., Refs. 4 and 7. For these simple dynamics, the optimal regulator feedback gains can be determined as explicit functions of K and $\dot{\delta}_M/\theta_M$ through the solution of the "root square equation."[8] These gains, in turn, lead to a dynamic compensator (the pilot) that we represent as Y_p in Fig. 1.

With $a=\dot{\delta}_M/\theta_M$, these are

for $Y_{c_1}=K$,

$$Y_p=\delta/\theta=a/s \tag{3}$$

for $Y_{c_2}=K/s$,

$$Y_p=0.707\left(\frac{a}{K}\right)^{1/2}\frac{1}{[0.707(aK)^{-1/2}]s+1} \tag{4}$$

and for $Y_{c_3}=K/s^2$,

$$Y_p=0.5\left(\frac{a^2}{K}\right)^{1/3}\frac{[2(aK)^{-1/3}]s+1}{[0.5(aK)^{-1/3}]s+1} \tag{5}$$

Turning our attention now toward the selection of $\dot{\delta}_M/\theta_M$, we assign an arbitrary maximum allowable deviation to the time rate of change of error $\dot{\theta}(t)$ and denote it $\dot{\theta}_M$. Now an "effective time constant" T can be introduced to define maximum allowable deviations of the integral and derivatives of $\dot{\theta}_M$ as

$$\begin{aligned}
&\theta_M=\dot{\theta}_M T\\
&\dot{\theta}_M=\text{specified but arbitrary}\\
&\ddot{\theta}_M=\dot{\theta}_M/T\\
&\dddot{\theta}_M=\ddot{\theta}_M/T=\dot{\theta}_M/T^2
\end{aligned} \tag{6}$$

$$\vdots$$

The justification for using a single time constant to represent the ratio of the maximum allowable value of a variable to that of its next highest derivative will be presented in the following discussion.

In a manner similar to Eq. (6), we write

$$\begin{aligned}
&\delta_M=\dot{\delta}_M T\\
&\dot{\delta}_M=\text{to be selected}\\
&\ddot{\delta}_M=\dot{\delta}_M/T\\
&\dddot{\delta}_M=\ddot{\delta}_M/T=\dot{\delta}_M/T^2
\end{aligned} \tag{7}$$

$$\vdots$$

The value of $\dot{\delta}_M$ is not arbitrary, however, but is found using Eqs. (6) and (7) and the vehicle dynamics as follows. Let Eqs. (2) be written as

$$Y_{c_i}=\theta/\delta=K/s^n, \qquad n=0,1,2$$

or, in the time domain,

$$d^n\theta/dt^n=K\delta \tag{8}$$

Use Eqs. (6-8) to develop the following relation between $\dot{\delta}_M$ and θ_M

$$\dot{\theta}_M/T^{n-1}=K\dot{\delta}_M T \tag{9}$$

or

$$\dot{\delta}_M=(1/KT^n)\cdot\dot{\theta}_M=\theta_M/KT^{n+1}$$

Now let

$$a=\dot{\delta}_M/\theta_M=1/KT^{n+1} \tag{10}$$

Equation (10) can be generalized to vehicles whose attitude transfer functions are expressed as the ratios of polynomials rather than simple free poles. Consider

$$\frac{\theta}{\delta}(s)=\frac{K[s^m+a_{m-1}s^{m-1}+\ldots+a_1s+a_0]}{[s^n+b_{n-1}s^{n-1}+\ldots+b_1s+b_0]} \tag{11}$$

Then, similar to Eq. (10) write

$$a=\frac{\dot{\delta}_M}{\theta_M}=\frac{[1/T^{n-1}+|b_{n-1}|/T^{n-2}+\ldots+|b_1|+|b_0|T]}{TK[1/T^{m-1}+|a_{m-1}|/T^{m-2}+\ldots+|a_1|+|a_0|T]} \tag{12}$$

The introduction of absolute values in Eq. (12) prevents singularities from occurring in the definition of $\dot{\delta}_M/\theta_M$. These can arise when vehicles with nonminimum phase dynamics are analyzed.

By using the relationship between the "gain" (a^2) defined on the root square locus[8] and the location of the highest-frequency closed-loop pole(s) in the optimal system, one can show that

$$\omega_B\simeq(Ka)^{1/(n-m+1)} \tag{13}$$

where ω_B is the bandwidth of the closed-loop system. Here, bandwidth is defined as the magnitude of that closed-loop pole closest to the frequency where $|\theta/\theta_c|$ is 6 dB below its zero frequency value. If more than one frequency meets this criterion, we choose the highest one. Equation (13) becomes increasingly exact as the ratio of weighting coefficients (a^2) increases in magnitude.

For the vehicle dynamics of Eqs. (2), and using Eqs. (6-10), Eq. (13) takes the very simple form

$$\omega_B\simeq 1/T \tag{14}$$

i.e., the closed-loop bandwidth is approximated by the reciprocal of the effective time constant. Table 1 demonstrates the utility of the preceding technique using the dynamics of Eq. (2) and the Y_p of Eqs. (3-5) with $K=1$ and $T=0.2$ s. Also shown in the last row of Table 1 are unstable vehicle dynamics of the form $Y_c=1/s(s-1)$. The reason for including these dynamics will be explained in the following section. For the unstable dynamics, application of Eqs. (6), (7), and (11-13) yields

$$\omega_B\simeq a^{1/3}=[(T+1)/T^3]^{1/3}=5.31 \text{ rad/s}$$

Table 1 indicates that, for the dynamics and effective time constant selected, Eq. (13) can be considered nearly exact. It is also interesting to note that, with T remaining *constant*, the bandwidth ω_B varies only slightly but the ratio of the weighting coefficients (a^2) varies by a factor of 900. These results are interesting as they suggest a *direct means* of selecting weighting coefficient values to obtain an optimal

Table 1 Optimal closed-loop charactersitics for stereotype vehicle dynamics

Y_c	T, s	a, 1/s	$\frac{\theta}{\theta_c}=\frac{Y_pY_c}{1+Y_pY_c}$	ω_B, rad/s	$(Ka)^{1/(n-m+1)}$, rad/s
1	0.2	5.0	$\frac{5}{(s+5)}$	5.0	5.0
1/s	0.2	25.0	$\frac{25}{(s^2+7.07s+25)}$	5.0	5.0
$1/s^2$	0.2	125.0	$\frac{5(s+2.5)}{(s+5)(s^2+5s+25)}$	5.0	5.0
$1/s(s-1)$	0.2	150.0	$\frac{68.2(s+2.19)}{(s+5.35)(s^2+5.33s+28.0)}$	5.35	5.31

control system with a desired bandwidth. The results are a direct consequence of the introduction of Eqs. (6-12) and justify the use of these equations in such analyses.

Pilot Modeling

In Ref. 3, the author demonstrates that the preceding technique for selecting index-of-performance weighting coefficients for an optimal regulator is applicable to the regulator part of the OCM as applied to the modeling of the human pilot. Since the estimator dynamics make *some* contribution to the form of Y_p, the approximation of Eq. (13) may be less exact than when applied to pure regulator designs at similar values of a.

Using the OCM and the four vehicle dynamics of Table 1, the analysis of Ref. 3 shows how human operator describing functions are generated that closely match those obtained from experiments. Here, we wish to generalize and simplify that modeling formulation, while still allowing the OCM to generate pilot models of sufficient accuracy to be of use in the engineering analysis of single-axis systems such as those to be discussed in the next section. Note that the unstable dynamics were included in Table 1, since they were used in Ref. 3 to validate the OCM technique.

To enhance the engineering utility of the OCM, the noise and disturbance characteristics associated with the estimator design were deliberately eliminated as analytical *variables*. To this end, noise covariances were set to values representative of those used in modeling the human operator in single-axis tracking tasks and were not varied in the analysis. In analyzing vehicle/control system configurations for any one data source (e.g., Ref. 2), disturbance intensities and bandwidths were invariant.

The technique for selecting the appropriate value of the effective time constant is discussed in some detail in Ref. 3 and will be only outlined here. In terms of the human pilot activity that we are modeling with the OCM, small values of T yield closed-loop systems with large bandwidths, good performance but high workload in terms of control activity. Conversely, large values of T yield closed-loop systems with small bandwidths, poor performance, but low workload in terms of control activity. This relationship between bandwidth and control activity is clear from Eqs. (11-13) for the optimal regulator, and the dependence of performance on adequate bandwidth is well known. Thus, selection of T by the analyst using the OCM seems to parallel a tradeoff between workload and performance that the human pilot makes in adopting particular dynamics (static gain, equalization, etc.) in controlling a vehicle. The technique used in Ref. 3 for selecting the appropriate value of T was graphical in nature. The value of the index of performance obtained from the OCM was plotted vs log $(1/T)$. The domain of the abscissa $\log(1/T)$ was selected with the midpoint defined as $\log(1/\tau_p)$ where τ_p represents the value of the pilot's time delay as utilized in the OCM formulation.[4] A nominal value of 0.2 s was used in Ref. 3 and retained in this analysis. Now the appropriate value of the effective time constant was chosen as the one corresponding to the "knee" of the curve just defined.

The technique just outlined needs to be modified slightly when time delays other than the pilot's exist in the forward loop of Fig. 1. Since the analysis of a linear system is not affected by the location of a time delay in the forward loop, rather only its magnitude, time delays associated with control law computation, effective delays associated with the phase effects of high-frequency structural suppression filters, etc., can simply be added to the pilot's time delay. Thus, in the method for selecting the effective time constant T, we consider the midpoint of the domain of $1/T$ to be defined as $\log[1/(\tau_p+\tau_D)]$. Here τ_D represents additional real or effective delays that exist in the vehicle/control system dynamics. The precise definition of τ_D as an effective delay can obviously be the subject of debate. In this analysis, we have chosen to borrow upon the results of extensive research in aircraft-equivalent systems (e.g., Ref. 9) and define τ_D as the delay that results when the actual higher-order aircraft/control system dynamics are fit to a transfer function of the form

$$\frac{\theta}{\delta}=\frac{K_\theta(T_\theta s+1)e^{-\tau_D s}}{s[s^2/\omega_n^2+(2\zeta_n/\omega_n)s+1]} \tag{15}$$

over a sufficiently broad frequency range. Note that Eq. (15) needs to be used only to define T via the graphical technique just outlined. If the analyst desires, the actual vehicle/control system dynamics can be used in generating the OCM itself. Such a course of action might be appropriate if the overall fit obtained by Eq. (15) is viewed as marginally acceptable.

As a brief aside, the author has found in analyzing a variety of single-axis manual control tasks with the OCM that the results of the graphical determination of T can be approximated by the following simple relation:

$$T\cong 0.65(\tau_p+\tau_D) \tag{16}$$

Although not exercised in this analysis, Eq. (16) offers a useful approximation for many engineering analyses of man/machine systems and obviates the time-consuming graphical procedure discussed in Ref. 3.

In the next section we show the results of employing the modeling technique just described to predict the open-loop longitudinal pilot/vehicle characteristics (Y_pY_c) for nine aircraft configurations evaluated in four different flight test experiments. Since the modeling procedure depends only upon the inner-loop vehicle/control system characteristics, the effects of specific outer-loop flight tasks (e.g., air-to-air tracking vs landing approach) are not pertinent. This is analogous to asking the pilot to maximize his performance in

attitude regulation regardless of whether the particular outer-loop task at hand requires such performance.

Examples

Figure 2 shows the longitudinal open-loop pilot/vehicle characteristics (including control system) for three of the configurations used in Ref. 2. The NASA Dryden F-8 digital fly-by-wire aircraft is considered with a rudimentary augmentation system ("pitch direct") and three real time delays of 0.13, 0.23, and 0.33 s. The predicted effect of the time delays is apparent in the reduced open-loop crossover frequencies ω_c. As Fig. 2 indicates, ω_c is defined as the frequency where $|Y_p Y_c| = 1.0$.

Similar results are also obtained for configurations from Ref. 10 as described in Ref. 11. Here, the NT-33A variable stability aircraft was used. Figure 3 compares a pair of open-loop transfer functions obtained using configurations 11 and 12 from Ref. 10. Once again, the dramatic difference in the crossover frequencies is apparent. Of particular interest here is the fact that no vehicle time delays, real or effective, were present in either configuration.

Figure 4 shows the predicted $Y_p Y_c$ for a pair of configurations from Ref. 12. In this study, the Princeton Variable Response Aircraft was used. The variable of interest here was again the amount of time delay in the control system. In the first, a delay of 0.055 s was employed, while in the second 0.355 s was used. Again, note the striking difference in the crossover frequencies.

Finally, Fig. 5 shows the predicted $Y_p Y_c$ for configurations 4-1 and 6-1 from Ref. 13. Again, the NT-33A variable stability aircraft was used. These configurations differ from previous examples in that the actual higher-order dynamics of the vehicle/control system were represented by the equivalent system of Eq. (15). The actual vehicle/control system dynamics were utilized in generating the OCM, however. As the figure indicates, configuration 6.1 exhibited a significantly lower crossover frequency than configuration 4.1.

Handling Qualities Implications

Two interesting phenomena are predicted in the pilot/vehicle characteristics of Figs. 2-5, one of which has already been pointed out. By varying the vehicle/control system dynamics it is apparently possible to dramatically reduce the open-loop crossover frequency (termed ω_c regression) and *also* to create a fair stretch of frequency beyond crossover where the slope of the $Y_p Y_c$ amplitude curve is considerably less than the "desirable," -20 dB/dec. This latter phenomenon would imply pilot lead equalization over and above that necessary to obtain K/s-like $Y_p Y_c$ characteristics. Both of these phenomena can combine to have deleterious effects on vehicle handling qualities.

While not necessarily a harbinger of dramatic deterioration in *disturbance* regulation (the task modeled here), ω_c regression can cause discrete command-following performance to suffer considerably. The first of these statements is analytically verified by considering the model-generated tracking scores for two of the F-8 configurations of Fig. 2. The 154% increase in time delay between the $\tau_D = 0.13$ and 0.33 s cases involved a log ω_c regression of nearly a decade. However, the predicted root mean square (rms) pitch attitude error increases by only 36% and predicted rms control rate actually decreases. However, an examination of closed-loop command-following characteristics (e.g., to a step θ_c), using the predicted $Y_p Y_c$ dynamics for configurations exhibiting ω_c regression, indicates poor transient performance as compared to configurations where regression did not occur. An approximate, but very simple, way to demonstrate this is to consider the integral of the error to a unit step command. It can be shown that, for unit step commands[14]

$$\int_0^\infty \theta_e(t)\,dt = 1/K_v$$

where K_v is the static velocity error coefficient. With a simple crossover model representation of $Y_p Y_c$ (discussed in the next section), one can further show

$$1/K_v \simeq 1/\omega_c$$

Thus, the integral of the step response error is inversely proportional to the open-loop crossover frequency, and the effect of ω_c regression is clearly evident.

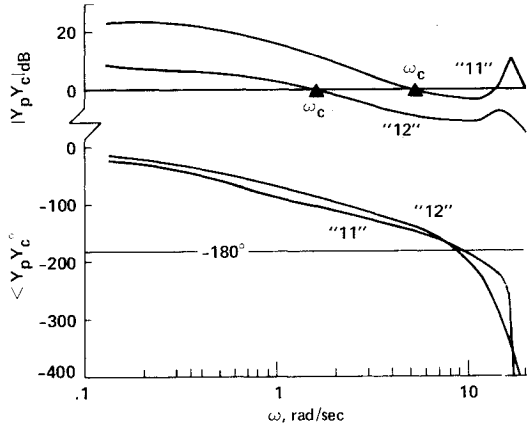

Fig. 3 Predicted pilot/vehicle dynamics ($Y_p Y_c$) for two configurations from Ref. 10.

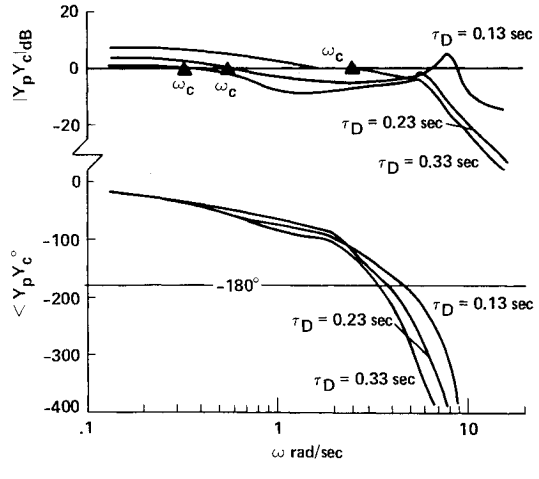

Fig. 2 Predicted pilot/vehicle dynamics ($Y_p Y_c$) for three-configurations from Ref. 2.

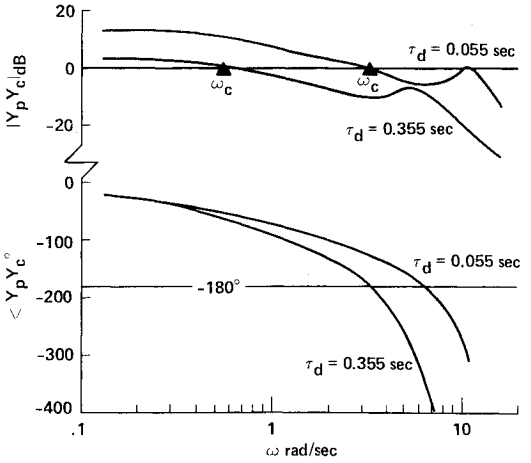

Fig. 4 Predicted pilot/vehicle dynamics ($Y_p Y_c$) for two configurations from Ref. 12.

A deterministic command might be internally generated by the pilot as an attitude command to correct an altitude error. This is indicated by the dashed signal path in Fig. 1. This deficiency in tracking discrete or abrupt commands has the potential for catalyzing pilot-induced oscillations when combined with the flat $Y_p Y_c$ amplitude characteristics beyond crossover. Recorded pilot comments (e.g., Ref. 2) indicate that the initial pilot reaction to poor transient performance often is an increase in static gain. With low ω_c values and relatively flat $Y_p Y_c$ amplitudes, a modest but abrupt static gain increase can cause the relatively large and adequate phase margins evident in Fig. 2 to disappear with equal abruptness. The effect of this would be the sudden appearance of a lightly damped oscillation in the vehicle pitch attitude and path mode responses. Smith has indicated such a condition to be a necessary part of a PIO excitation.[15]

Consider Fig. 6, which demonstrates how closed-loop system damping is effected by an open-loop static gain increment of 5 dB for the $\tau_D = 0.33$ s case in the F-8 aircraft. A lightly damped closed-loop mode appears at 3.3 rad/s, which is nearly identical to the frequency of a pilot-induced oscillation that occurred in flight test at this delay. In the flight test of configurations 11 and 12 of Fig. 3, configuration 12 was rated PIO prone, while configuration 11 was not. In the two configurations of Fig. 4, the $\tau_D = 0.055$ s case showed no PIO tendencies, while the $\tau_D = 0.355$ s case produced PIOs. Finally, in the flight test of configurations 4.1 and 6.1 of Fig. 5, the former exhibited no PIO tendencies, while the latter produced a PIO with a frequency of approximately 3.5 rad/s. A 4.75 dB increase in the predicted pilot static gain for this configuration would produce a closed-loop instability at 3.75 rad/s, quite close to the actual PIO frequency.

In each of the cases just discussed, we have made a direct comparison of vehicles that were found to be PIO prone with those that were not. The hypothesis linking an aircraft's PIO tendencies to the predicted $Y_p Y_c$ characteristics seems to be corroborated by the data. However, some of the PIO-prone vehicles, particularly those represented in Figs. 2 and 4, tend to represent extreme cases in terms of time delays in the vehicle/control system dynamics. It would be useful if one could determine an approximate critical crossover frequency that could be used to separate aircraft that are PIO prone from those that are not. This is the subject of the next section.

A PIO Criterion

We will employ a crossover model[7] of the human pilot to study the effects of ω_c regresssion on closed-loop bandwidth. Since the crossover model hypothesizes K/s-like pilot/vehicle characteristics in and around the region of crossover (hence its name), it obviously will not exhibit the amplitude flattening predicted by the OCM when ω_c regresses. However, the model will provide a useful means for delineating a lower desirable limit for ω_c. The crossover model can be written as

$$Y_p Y_c = \omega_c e^{-\tau_e s}/s \tag{17}$$

The reader is cautioned that the τ_e value used in this model is not necessarily synonomous with the definition of any of the delays discussed previously. The τ_e is generally dependent upon the form of pilot equalization, disturbance bandwidth, etc. Representing τ_e by a first-order Padé approximation,

$$\tau_e \simeq -(s-2/\tau_e)/(s+2/\tau_e)$$

the closed-loop system transfer function can be given by

$$\frac{\theta}{\theta_c} = \frac{Y_p Y_c}{1+Y_p Y_c} = \frac{-\omega_c(s-2/\tau_e)}{s^2+(2/\tau_e-\omega_c)s+2\omega_c\tau_e} \tag{18}$$

Now for $\omega_c > 0.34/\tau_e$, the closed-loop characteristic roots of Eq. (18) are complex; for $\omega_c \leq 0.34/\tau_e$, they are real. Observing that the closed-loop bandwidth is the magnitude of the smallest closed-loop pole(s), let us consider $\partial\omega_B/\partial\omega_c$, i.e., the sensitivity of the closed-loop bandwidth to changes in the open-loop crossover frequency:

for $\omega_c > 0.34/\tau_e$,

$$\frac{\partial\omega_B}{\partial\omega_c} = (2\omega_c\tau_e)^{-1/2} \tag{19}$$

and for $\omega_c \leq 0.34/\tau_e$,

$$\frac{\partial\omega_B}{\partial\omega_c} = -0.5 - \frac{0.25(2\omega_c - 12/\tau_e)}{(\omega_c^2 - 12\omega_c/\tau_e + 4/\tau_e^2)^{1/2}} \tag{20}$$

For $\omega_c \leq 0.34/\tau_e$, ω_B becomes very sensitive to changes in ω_c. This becomes apparent by calculating the values of $\partial\omega_B/\partial\omega_c$ at $\omega_c = 0.34/\tau_e$ and evaluating the right-hand sides of both Eqs. (19) and (20). Equation (19) gives

$$\frac{\partial\omega_B}{\partial\omega_c} = 1.2$$

while from Eq. (20)

$$\frac{\partial\omega_B}{\partial\omega_c} = 14.4$$

Thus, $\omega_c = 0.34/\tau_e$ represents a reasonable lower limit for desirable ω_c, i.e., the value of ω_c below which ω_B becomes very sensitive to further decrements in ω_c. Since the critical value of ω_c is inversely proportional to τ_e, a conservative estimate of the latter quantity can be obtained by using a value of τ_e representative of the lower limit of such delays as reported in the literature. A value of 0.2 s is appropriate.[7] This leads to a critical value of ω_c of 1.7 rad/s.

Now the effects of amplitude flattening in the predicted $Y_p Y_c$ can be qualitatively assessed by considering a more accurate representation of $Y_p Y_c$ to be

$$Y_p Y_c = \frac{\omega_c e^{-\tau_e s}(T_1 s+1)(T_3 s+1)}{(T_2 s+1)(T_4 s+1)} \tag{21}$$

where $T_1 > T_2 > T_3 > T_4$. The effect of the additional poles and zeros in Eq. (21) is to flatten the amplitude characteristics of $Y_p Y_c$ as compared to that of Eq. (17). The closed-loop effect is to keep ω_B a good deal larger than it would be if amplitude flattening did not occur. However, this is done at the expense of having the closed-loop amplitude less than unity for a wide frequency range below ω_B. This is clearly evident in Fig. 6. It is interesting to note that the approximate relationship of Eq. (13) can still be shown to hold in Fig. 6. However, our definition of bandwidth is not as meaningful a measure of transient performance in the case of amplitude flattening because of the deleterious effects of the closed-loop amplitude attenuation. Nonetheless, the results of the preceding analysis ignoring amplitude flattening are still valid since, in that case, the definition of closed-loop bandwidth *is* a meaningful measure of transient performance.

We now state the following PIO criterion: if the maximum pilot/vehicle attitude crossover frequency consisent with adequate stability margins, and predicted by *any* valid pilot/vehicle analysis technique, lies within or below the frequency range of 1.5-2 rad/s, the vehicle under consideration should be suspected of being prone to pilot-induced oscillations.

Implicit in this criterion and the modeling work that preceded it is the assumption that adequate attitude bandwidth is essential for outer-loop path control and that such path control may require abrupt, transient attitude commands. Note that the criterion does not imply that pilot-induced oscillations will actually occur if $\omega_c \leq 1.5$-2 rad/s, only that an important *necessary* condition for PIO susceptibility has been met. Other conditions, such as the nature of normal acceleration cues at the pilot's station,

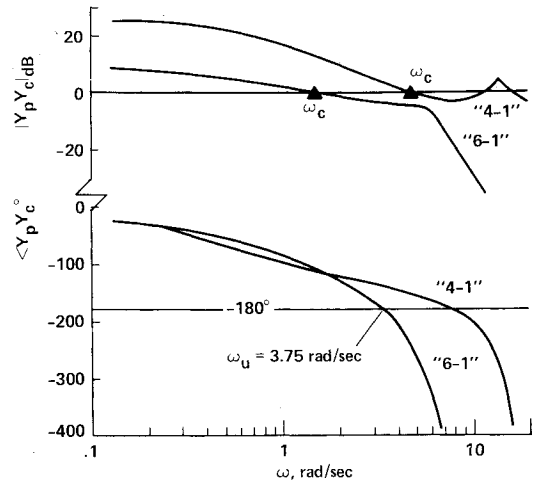

Fig. 5 Predicted pilot/vehicle dynamics (Y_pY_c) for two configurations from Ref. 13.

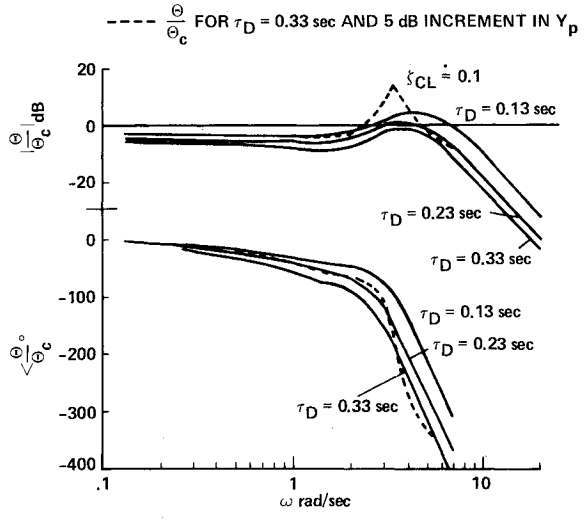

Fig. 6 Predicted closed-loop dynamics $[\theta/\theta_c = Y_pY_c/(1+Y_pY_c)]$ for three configurations from Ref. 2.

appear to influence the catalyzation and sustenance of PIOs.[15] Finally, it should be noted that the OCM technique, as used here, will not reflect handling qualities deficiencies that have their origins in improper control sensitivities. As Eq. (12) indicates, the control sensitivity K appears in the denominator of the relation defining the ratio of index-of-performance weighting coefficients. Thus, when the modeling procedure is applied to two vehicles whose dynamics differ only in the value of K, identical Y_pY_c characteristics will be predicted since changes in K are reflected in inversely proportional changes in the weighting on control rate. This is not a modeling deficiency, however, since experimental evidence indicates this is precisely what the human pilot does![7] Unlike our particular OCM, however, the human has a range of control sensitivities which he finds preferable. These are undoubtedly based upon the neuromuscular characteristics of the limb driving the control stick.

We now consider a final illustrative example in which the criterion is applied to an existing vehicle whose PIO tendencies have been exhaustively examined by others, namely the Shuttle Orbiter vehicle.

A Final Example

The attitude dynamics for the Shuttle Orbiter vehicle as flown in the fifth free-flight test are adequately represented

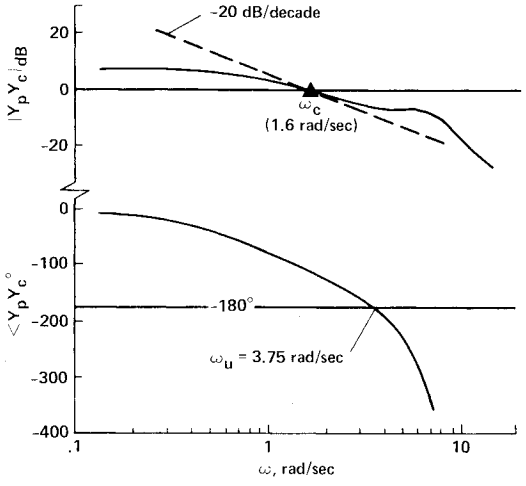

Fig. 7 Predicted pilot/vehicle dynamics (Y_pY_c) for Shuttle Orbiter configuration.

by[16]

$$\frac{\theta}{\delta} = \frac{0.4e^{-0.264S}}{s(s/3.5+1)} \tag{22}$$

Equation (22) represents an equivalent system and its adequacy in the appropriate frequency region led to its use as the actual vehicle dynamics for this example.

Figure 7 shows the predicted Y_pY_c characteristics obtained using the OCM modeling technique discussed in the preceding sections. Note that the predicted crossover frequency of 1.6 rad/s falls within the criterion range and that Y_pY_c exhibits the amplitude flattening evident in the analyses of other PIO-prone vehicles. This last fact has been emphasized in Fig. 7 by showing a dashed line at -20 dB/s for comparison. As is well known, the Shuttle Orbiter did experience a serious longitudinal PIO in its fifth free-flight test.[16,17] The approximate frequency of the oscillation was 3.5 rad/s, which compares favorably with the predicted unstable frequency here of $\omega_u = 3.75$ rad/s shown in Fig. 7. This instability would occur with a 5 dB increase in predicted pilot static gain.

Conclusions

Based upon the foregoing analysis, the following conclusions can be drawn:

1) A straightforward technique for generating models of the human pilot in single-axis tracking tasks has been offered. The technique is based upon a novel method for selecting optimal control model index-of-performance weighting coefficients based *solely* upon the characteristics of the vehicle dynamics and the value of the pilot's time delay as used in the optimal control model.

2) The vehicle dynamics can have a dramatic effect upon both the open-loop pilot/vehicle crossover frequency and the nature of the pilot equalization as predicted by the pilot modeling technique. This is particularly true when the vehicle dynamics contain real or effective time delays. The latter are often the result of higher-order vehicle dynamics.

3) Given the predicted pilot/vehicle characteristics obtained from the pilot modeling technique, a simple criterion for assessing an aircraft's susceptibility to pilot-induced oscillations can be developed using a simple crossover model of the human pilot.

Acknowledgment

The major portion of this research was completed while the author was with the Aircraft Guidance and Navigation Branch, NASA Ames Research Center, Moffett Field, Calif.

References

[1]"Military Specification, Flying Qualities of Piloted Airplanes," MIL-F-8785B(ASG), Aug. 1969.

[2]Berry, D.T., Powers, B. G., Szalai, K.J., and Wilson, R.J., "In-Flight Evaluation of Control System Pure Time Delays," *Journal of Aircraft,* Vol. 19, April 1982, pp. 318-323.

[3]Hess, R.A., "A Pilot Modeling Technique for Handling Qualities Research," AIAA Paper 80-1624, 1980.

[4]Kleinman, D.L., Baron, S., and Levison, W.H., "An Optimal Control Model of Human Response," Pts. I and II, *Automatica,* Vol. 6, May 1970, pp. 357-369.

[5]Curry, R.E., Kleinman, D.L., and Hoffman, W.C., "A Design Procedure for Control Display Systems," *Human Factors,* Vol. 19, No. 5, Oct. 1977, pp. 437-458.

[6]Bryson, A.E., *Applied Optimal Control,* Blaisdell, Waltham, Mass., 1969, Chap. 5.

[7]McRuer, D.T., Graham, D., Krendel, E., and Reisener, W. Jr., "Human Pilot Dynamics in Compensatory Systems," AFFDL-TR-65-15, July 1965.

[8]Rynaski, E.G. and Whitbeck, R.F., "The Theory and Application of Linear Optimal Control," AFFDL-TR-65-28, Jan. 1966.

[9]Hodgkinson, J., "Equivalent Systems Criteria for Handling Qualities of Military Aircraft," *Criteria for Handling Qualities of Military Aircraft,* AGARD Conference Proceedings, No. 333, June 1982, pp. 3-1—3-11.

[10]Neal, P.T. and Smith, R.E., "An In-Flight Investigation to Develop Control System Design Criteria for Fighter Airplanes," AFFDL-TR-70-74, Dec. 1970.

[11]Arnold, J.D., "An Improved Method of Predicting Aircraft Longitudinal Handling Qualities Based on the Minimum Pilot Rating Concept," Air Force Institute of Technology, Rept. GGC/MA/73-122, 1973.

[12]Stengel, R.F. and Miller, G.E., "Flight Tests of a Microprocessor Control System," *Journal of Guidance and Control,* Vol. 3, Nov.-Dec. 1980, pp. 494-500.

[13]Smith, R.E., "Effects of Control System Dynamics on Fighter Approach and Landing Longitudinal Flying Qualities," Vol. 1, AFFDL-TR-73-122, 1978.

[14]Ogata, K., *Modern Control Engineering,* Prentice-Hall, Englewood Cliffs, N.J., Chap. 7.

[15]Smith, R.H., "A Theory for Longitudinal Short-Period Pilot Induced Oscillations," AFFDL-TR-77-57, June 1977.

[16]Ashkenas, I., "Space Shuttle PIO Analysis," presented at NASA-Air Force Workshop on Pilot Induced Oscillations," NASA Dryden Flight Research Center, Nov. 1980.

[17]Powers, B.G., "An Adaptive Stick-Gain to Reduce Pilot Induced Oscillation Tendencies," *Journal of Guidance, Control, and Dynamics,* Vol. 5, March-April 1982, pp. 138-142.